Gemi ve Deniz Teknolojisi Dergisi
Sayı: 221, Haziran 2022
ISSN: 1300-1973, e-ISSN: 2651-530X, Dergi ana sayfası: http://www.gmoshipmar.org/
Araştırma Makalesi

Dönebilir İticinin Sert Hava Koşullarında Bir Balıkçı Gemisinin Manevra Kabiliyetine Etkisi

Ömer Kemal Kınacı [1], Kadir Sarıöz [2], Ömer Gören [3], Aydin Sülüs [4]

[1,2,3] Gemi İnşaatı ve Deniz Bilimleri Fakültesi, İstanbul Teknik Üniversitesi, İstanbul, Türkiye
[4] Skipsteknisk Mühendislik AŞ, Maltepe, İstanbul, Türkiye

[1] (sorumlu yazar), kemalkinaci@gmail.com, ORCID: 0000-0002-2956-9562
[2] sarioz@itu.edu.tr, 0000-0001-9594-4677
[3] ogoren@itu.edu.tr, 0000-0002-0413-7376
[4] aydin.sulus@skipsteknisk.no, 0000-0000-0000-0000

ÖZET

Bu çalışmada; bir balıkçı gemisinin baş tarafında yer alan dönebilir iticinin, gemi manevra performansına etkileri hesaplamalı olarak incelenmiştir. Tek şaftlı, pervaneli ve dümenli geminin ilk tasarımının, 40 ton yüklü durumda ve 3 knot ilerleme hızı ile orta çevre koşullarında manevra performansı yetersiz bulunmuştur. Modifiye edilmiş tasarım, geminin baş tarafında yer alan ve ilave itme kuvveti üretmek için 360 derece dönebilen bir azimut pervanesi ile donatılmıştır. Geminin manevra performansını değerlendirmek için 3 serbestlik dereceli nonlineer gemi hareket denklemleri zaman düzleminde çözülmüştür. Kullanılan matematiksel modelin manevra katsayıları iki farklı yaklaşımla tahmin edilmektedir; birincisi yarı ampirik yöntemlere, diğeri ise hesaplamalı akışkanlar dinamiğine (HAD) dayanmaktadır. Rüzgâr, akım ve dalga gibi dış bozucular, yarı ampirik yöntemlerle matematiksel olarak temsil edilmiştir. Kapsamlı bir hesaplamalı test matrisi oluşturulmuş ve bir balıkçı teknesinin baş tarafına yerleştirilmiş yeterli itme gücüne sahip bir azimut pervanesinin olumsuz çevresel koşullara rağmen geminin manevra performansını önemli ölçüde iyileştirebileceği simülasyonlarla gösterilmiştir.

Anahtar kelimeler: Manevra performansı, balıkçı gemisi, azimut, dönebilir itici

Makale geçmişi: Geliş 26/04/2022 – Kabul 25/06/2022

https://doi.org/10.54926/gdt. 1108980

GMO Journal of Ship and Marine Technology
Issue: 221, June 2022
ISSN: 1300-1973, e-ISSN: 2651-530X, Journal homepage: http://www.gmoshipmar.org/
Research Article

The Effect of Azimuth Thruster on the Manoeuvring Ability of a Stern Trawler in Rough Weather Conditions

Ömer Kemal Kınacı [1], Kadir Sarıöz [2], Ömer Gören [3], Aydin Sülüs [4]

[1,2,3] Faculty of Naval Architecture and Ocean Engineering, Istanbul Technical University, Istanbul, Türkiye
[4] Skipsteknisk Engineering AŞ, Maltepe, Istanbul, Türkiye

[1] (correnponding author), kemalkinaci@gmail.com, ORCID: 0000-0002-2956-9562
[2] sarioz@itu.edu.tr, 0000-0001-9594-4677
[3] ogoren@itu.edu.tr, 0000-0002-0413-7376
[4] aydin.sulus@skipsteknisk.no, 0000-0000-0000-0000

ABSTRACT

The results of computational analyses on the manoeuvring performance of a stern trawler with an azimuth thruster located in the forward part of the vessel are presented. The initial design of the vessel with a single shaft, propeller and rudder is considered to have insufficient manoeuvring performance with a trawl pull load of 40 tons in moderate environmental conditions with a forward speed of 3 knots. The modified design is equipped with an azimuth thruster located in the forward part of the vessel that can rotate 360 degrees to produce additional thrust. In order to assess and simulate the manoeuvring performance of the vessel, the surge, sway and yaw equations are set and solved in the time domain. The hydrodynamic forces due to surge and sway motions and the yaw moment are represented by a nonlinear modular mathematical model. The manoeuvring coefficients of the mathematical model employed are estimated by two distinct approaches; the first one is based on semi-empirical methods and the other is based on computational fluid dynamics (CFD). The external forces due to wind, current and waves are mathematically represented by proven semi-empirical methods based on the results of scaled model tests and full-scale measurements. A comprehensive computational test matrix is established and extensive computational analyses and manoeuvring simulations were carried out to indicate that an azimuth thruster with sufficient thrust located in the forward part of a stern trawler could significantly improve the manoeuvring performance of the vessel despite adverse environmental conditions.

Keywords: Maneuvering performance, stern trawler, azimuth thruster

Article history: Received 26/04/2022 – Accepted 25/06/2022

1. Introduction

Modern stern trawlers are designed for hauling very heavy catches up the stern onto the working deck of the vessel under adverse environmental conditions. Although it is asserted in some studies, such as Yoshimura and Ma (2003), that fishing vessels generally have good performances in manoeuvrability because of large rudders and powerful propeller assists, under particular operational and environmental conditions manoeuvrability may turn out to be a problem. Thus, the present study attempted to take severe environmental conditions into account as well as slow speed in the trawling mode of the vessel's operation. The weight of huge nets not only require powerful engines but also additional manoeuvring devices – such as azimuth thrusters – which may be needed to provide sufficient manoeuvring performance in higher sea states. Another difficulty is due to the slow forward speed to be maintained while pulling the net which reduces the efficiency of the rudder.

In this paper the influence of an azimuth thruster on the manoeuvring performance of astern trawler is investigated. The stern trawler under investigation is designed by Skipsteknisk. The initial design, Base Case (0), is fitted with a single shaft/propeller and a rudder. The modified design, Base Case (1), is additionally equipped with an azimuth thruster located in the forward part of the vessel that can rotate 360 degrees to produce additional thrust. The manoeuvring performance of these configurations with a trawl pull load of 40 metric tons is assessed and simulated in calm water and moderate to extreme environmental conditions. For each configuration the following conditions are considered:

- Forward speed of 3 knots,
- Trawl pull load of 40 metric tons,
- Wave, wind and a 3 knot current acting on the vessel in beam direction.

In order to assess and simulate the manoeuvring performance of the vessel, surge, sway and yaw equations are set and solved in the time domain. The hydrodynamic forces due to surge and sway motions and the yaw moment are represented by a set of linear and nonlinear coefficients called the manoeuvring derivatives. These coefficients may be estimated by empirical methods, CFD (Computational Fluid Dynamics) based computational procedures or PMM (Planar Motion Mechanism) model tests. It is a known fact that most of the empirical formulas have been derived from the model tests of merchant ships and from the analytical studies of some particular geometrical shapes. In order to have a good correlation between hull form parameters – employed in the empirical formulas – and the manoeuvring derivatives, Kim et al. (2021) recently introduced modified empirical formulas developed for fishing vessels of which hull form characteristics are different from those of merchant ships. In the present study, we prefer to go through the CFD analyses in calculating manoeuvring derivatives, as well, to validate the results of empirical formulas.

Section 2 presents the equations of motion and describes the modular mathematical manoeuvring model including the external forces due to the propeller, thruster, rudder and environmental disturbances such as wind, current and waves to be separately estimated and included in the equations of the motion. The propeller forces are estimated by considering the experimental open water efficiency and the thrust deduction data provided by the designer of the vessel. Thrust reduction due to currents, thruster-hull interaction and ventilation effects are taken into consideration by using suitable empirical methods. The forces and moment due to the rudder are estimated by a well proven empirical method which takes into account the effects of propeller flow on the rudder and the effective

ISSN: 1300-1973, e-ISSN: 2651-530X, Journal homepage: http://www.gmoshipmar.org/
Research Article

rudder angle in a turn. Methods and procedures used to estimate propeller and thruster forces and forces and moment due to the rudder are also presented.

The empirical methods employed and the CFD based computations performed to estimate the manoeuvring derivatives are explained in Section 3.

Turning performance of the Stern Trawler in calm water conditions is presented in Section 4. In Base Case (0) configuration, only the propeller and rudder are taken into consideration and the effect of a trawl pull load of 40 metric tons on turning performance of the vessel is illustrated. In Base Case (1) configuration, the effect of an azimuth thruster on turning performance in calm water is investigated.

Section 5 presents the methods used to estimate the external forces due to wind, current and waves. As shown in this section several alternative empirical methods are available to estimate the environmental forces. It is shown that the forces and moment predicted by these methods are, generally, in agreement and result in similar manoeuvring behaviour.

Manoeuvring performance of the stern trawler in a range of environmental conditions in Base Case (0) and Base Case (1) configurations are presented and compared in Section 6. Based on these analyses, maximum environmental conditions in which the vessel could maintain the track are estimated in Section 7. The paper ends with a summary of the results and the concluding remarks.

2. The Mathematical Model

The mathematical model to simulate the motions of the ship is the modular MMG mathematical ship manoeuvring model (Yasukawa and Yoshimura, 2015). This model considers the ship hull and its appendages separately and the interaction between them is handled by various parameters. In this section, we first present the ship manoeuvring equations used in this study and then briefly present the models used for the ship hull and its appendages (the propeller, the azimuth thruster and the rudder).

2.1. Equations of motion

Assuming that the effect of roll on the manoeuvring motion is small, only surge, sway and yaw motions are considered in the equations of motion which can be expressed as follows with respect to a ship fixed reference frame at amidships:

$$\begin{aligned} X &= m(\dot{u} - vr - x_G r^2) \\ Y &= m(\dot{v} + ur + x_G \dot{r}) \\ N &= I_z \dot{r} + m x_G (\dot{v} + ru) \end{aligned} \tag{1}$$

m : ship's mass

I_z : mass moment of inertia of the ship about the vertical axis

X : total force in the x direction

Y : total force in the y direction

N : turning moment around the vertical axis

u : velocity component in the x direction

v : velocity component in the y direction

r : yaw rate

x_G : the distance between the midships and the centre of gravity.

The main components of the external forces are:

- Hydrodynamic forces due to the surrounding fluid (X_F, Y_F, N_F),
- Control surface forces due to control surfaces like rudder and fins(X_R, Y_R, N_R),
- Propulsion forces due to the propellers and thrusters(X_T, Y_T, N_T),
- Environmental disturbances such as wind, current and waves(X_E, Y_E, N_E),
- External forces due to trawl pull loads (X_P, Y_P, N_P).

Then the equations of motion can be written as follows;

$$m(\dot{u} - vr - x_G r^2) = X_F + X_R + X_T + X_E + X_P$$

$$m(\dot{v} + ur + x_G \dot{r}) = Y_F + Y_R + Y_T + Y_E + Y_P$$

$$I_z \dot{r} + m x_G (\dot{v} + ru) = N_F + N_R + N_T + N_E + N_P$$

X_F, Y_F, N_F : Hydrodynamic forces due to the surrounding fluid,

X_R, Y_R, N_R : Control surface forces due to the rudder and fins,

X_T, Y_T, N_T : Propulsion forces due to the propeller and thrusters,

X_E, Y_E, N_E : Environmental loads due to wind, current and waves,

X_P, Y_P, N_P : External forces due to pull loads such as trawl nets,

2.2. Forces and moment acting on the ship hull

The hydrodynamic forces and moments can be considered as sums of various components with different static and dynamic origins, as follows:

- Added mass and moment components due to the motion in an ideal fluid with no circulation,
- Lift force and moment components due to the motion in an ideal fluid with circulation,
- Viscous force and moment components due to the motion in a viscous fluid.

The hydrodynamic forces due to surge and sway motions and the yaw moment are represented by a set of linear and nonlinear hydrodynamic coefficients. These coefficients may be estimated by empirical methods, CFD based computational procedures or PMM model tests. For the manoeuvring simulations presented in this report, the cubic model for equations of motion is adopted and the manoeuvring derivatives obtained by CFD computations are used with the exception of inertia coefficients. Hydrodynamic forces due to the surrounding fluid are expressed as follows:

Methods and procedures used to estimate the forces due to the propeller and thrusters, rudder and environmental disturbances such as wind, current and waves are explained in the following subsections.

ISSN: 1300-1973, e-ISSN: 2651-530X, Journal homepage: http://www.gmoshipmar.org/
Research Article

$$X_F = \frac{\rho}{2}L^3(X'_{\dot{u}}\dot{u}) + \frac{\rho}{2}L^2(X'_{vv}v^2) + \frac{\rho}{2}L^3(X'_{vr}vr) + \frac{\rho}{2}L^4(X'_{rr}r^2)$$

$$Y_F = \frac{\rho}{2}L^3(Y'_{\dot{v}}\dot{v}) + \frac{\rho}{2}L^4(Y'_{\dot{r}}\dot{r}) + \frac{\rho}{2}L^2(Y'_{v}uv) + \frac{\rho}{2}L^3(Y'_{r}ur) + \frac{\rho}{2}L^2(Y'_{vvv}v^3) + \frac{\rho}{2}L^3(Y'_{vvr}vvr + Y'_{vrr}vrr) + \frac{\rho}{2}L^4(Y'_{rrr}r^3) \quad (2)$$

$$N_F = \frac{\rho}{2}L^4(N'_{\dot{v}}\dot{v}) + \frac{\rho}{2}L^5(N'_{\dot{r}}\dot{r}) + \frac{\rho}{2}L^3(N'_{v}uv) + \frac{\rho}{2}L^4(N'_{r}ur) + \frac{\rho}{2}L^3(N'_{vvv}v^3) + \frac{\rho}{2}L^4(N'_{vvr}vvr + N'_{vrr}vrr) + \frac{\rho}{2}L^5(N'_{rrr}r^3)$$

2.3. Forces generated by the propeller

The manoeuvring model adopted in this study considers the propeller to generate only a force in the surge direction. Lateral forces or moments are ignored. In this case, the propeller net thrust force may be represented by

$$X_P = (1-t)\rho n_P^2 D_P^4 K_T(J_P) \quad (3)$$

where t is the thrust deduction fraction, n_P the propeller rotational rate and D_P the propeller diameter. The thrust coefficient $K_T(J_P)$ can be estimated by using the open water test measurements of the propeller as a function of the advance number J_P, which is expressed as:

$$J_P = \frac{u_P}{n_P D_P} = \frac{u(1-w_P)}{n_P D_P} \quad (4)$$

where u is the axial ship velocity and w_P is the Taylor wake fraction of the propeller behind the ship hull. In order to estimate the thrust coefficient $K_T(J_P)$ for a given advance number, J_P, the open-water test data of the propeller is utilized. The open water characteristics of the propeller are represented by a third-order polynomial. The speed of the vessel is limited to 3 knots while pulling the trawl net. At these low speeds, the wave-making resistance can be ignored and the total resistance may be assumed to be due to the viscous component only:

$$R_T \cong R_V = \frac{1}{2}\rho S u^2[(1+k)C_F + \Delta C_F] \quad (5)$$

Frictional resistance coefficient C_F is estimated by using the ITTC 1957 formula. At the self-propulsion condition the thrust is equal to the sum of the total resistance and the trawl pull, i.e., $X_P = X_R + F_P$. The trawl pull load F_P is 40 metric tons.

2.4. Forces and moment generated by the rudder

The components of the hydrodynamic forces acting on the rudder are essentially of the same category as for a ship hull, with an additional complication that the rudder forces are significantly dependent on the velocity of the propeller slip-stream. The true hydrodynamic description of rudder performance and its forces should be based on effective velocity over the rudder, (accounting for the race effect of the propeller), and the effective angle of attack on the rudder. The forces and moment generated by the rudder are (Inoue et al., 1981);

$$X_R = -F_N \sin\delta$$
$$Y_R = -(1 + a_H) F_N \cos\delta \quad (6)$$
$$N_R = -(1 + a_H) x_R F_N \cos\delta$$

where a_H is the ratio of additional lateral force, x_R and z_R are the x and z-coordinates of the centre of lateral force, δ is the rudder angle and F_N is the rudder normal force. The a_H coefficient can be estimated as a function of the block coefficient as follows, IMCA M140 (2000);

$$a_H = 0.62(C_B - 0.6) + 0.227 \quad (7)$$

The normal force on the rudder can be approximated as

$$F_N = \frac{\rho}{2} \frac{6.13\lambda}{\lambda + 2.25} A_R V_R^2 \sin\alpha_R \quad (8)$$

where A_R is the rudder area and λ is the effective aspect ratio. The effective rudder inflow speed can be expressed in the form

$$V_R = V(1 - w_R)\sqrt{1 + K_2 g(s)}$$
$$V = \sqrt{u^2 + v^2} \quad (9)$$

where u and v are the components of ship speed in x and y directions, respectively, $K_2 = 1.065$ for the port rudder and $K_2 = 0.935$ for the starboard rudder. The term $K_2\, g(s)$ represents the effect of the propeller slip-stream on V_R, and

$$g(s) = \eta\kappa[2 - (2 - \kappa)s]s/(1 - s)^2$$
$$s = 1 - u(1 - w_P)/nP$$
$$\eta = D_P/H_R \quad (10)$$
$$\kappa = 0.6(1 - w_P)/(1 - w_R)$$

where u is the longitudinal component of ship speed, D_P is the propeller diameter, P is the propeller pitch, H_R is the rudder height, n is the propeller revolution and, w_P and w_R are the effective propeller and rudder wake fractions, respectively. The estimation of the effective rudder wake fraction is made assuming that w_R in the manoeuvring motion could be computed by

$$\frac{w_R}{w_{RO}} = \frac{w_P}{w_{PO}} = \exp\left(K_1 \beta_P^2\right) \quad (11)$$

where $K_1 = -4.0$ and the geometrical inflow angle at the propeller position is defined as follows:

$$\beta_P = \beta - x_P' r' \quad (12)$$

The effective rudder wake fraction w_{RO} of full-scale ships may be obtained from the results of the model experiments in the same manner as for the effective propeller wake fraction w_{PO} in the area of the ship propulsion, namely making use of the technique to estimate the full-scale value from the

ISSN: 1300-1973, e-ISSN: 2651-530X, Journal homepage: http://www.gmoshipmar.org/
Research Article

model experimental results with the concept of the wake ratio. Taking the flow-rectifying effect into considerations, the effective rudder angle, α_R can be expressed in the form,

$$\alpha_R = \delta + \delta_O - \gamma\beta'_R$$
$$\beta'_R = \beta - 2x'_R r' \tag{13}$$

The flow rectifying effect due the ship's hull and the propeller can be expressed as,

$$\gamma = C_P C_S$$
$$C_P = 1/\sqrt{1 + 0.6\eta(2 - 1.4s)s/(1 - s)^2} \tag{14}$$

The ship flow-rectification coefficient $C_P$is given in the following form:

$C_S = K_3\beta'_R$ for $\beta'_R \leq C_{SO}/K_3$

$C_S = C_{SO}$ for $\beta'_R > C_{SO}/K_3$

with $K_3 = 0.45$ and $C_{SO} = 0.5$.

2.5. External disturbances – Wind loads

The wind force calculations are based on a steady state one-minute mean wind velocity measured at an elevation of 10 meters above the water surface. For wind velocities at different elevation, adjustments to the equivalent 10-meter velocity are necessary and can be made with the following formula; IMCA M140 (2000) and OCIMF 94 (1994);

$$V_w = v_w \left(\frac{10}{h}\right)^{1/7} \tag{15}$$

where V_w is the 10-meter wind velocity (m/s), v_w is the wind velocity at elevation h (m/s) and h is the elevation above water surface (m). Since the wind speed is subjected to gusts, the one-minute mean value is converted to the hourly mean value by multiplying by 1.15 (IMCA M140, 2000). The wind forces and moment can be estimated by using the following standard formulations, IMCA M140 (2000);

$$F_{Wx} = \frac{\rho_a}{2} V_{Wr}^2 A_T C_{Wx}(\alpha_{Wr})$$
$$F_{Wy} = \frac{\rho_a}{2} V_{Wr}^2 A_L C_{Wy}(\alpha_{Wr}) \tag{16}$$
$$N_W = \frac{\rho_a}{2} V_{Wr}^2 A_L L_{BP} C_{Wn}(\alpha_{Wr})$$

V_{Wr} is the instantaneous wind velocity including the ship's speed over the ground with the following longitudinal and transverse components:

$$V_{Wx} = V_W \cos\alpha_W - u$$
$$V_{Wy} = V_W \sin\alpha_W - v \tag{17}$$
$$V_{Wr} = \sqrt{V_{Wx}^2 + V_{Wy}^2}$$

Then, the relative wind direction, i.e. the angle between the speed through the water and the ships heading can be expressed as follows:

$$\alpha_{Wr} = \arctan\left(V_{Wy}/V_{Wx}\right) - \psi \tag{18}$$

where ψ is the heading of the vessel. The coefficients C_{Wx}, C_{Wy} and C_{Wn} are calculated using IMCA M140 (2000).

2.6. External disturbances – Current loads

The current forces and moment can be estimated by using the following standard formulations:

$$\begin{aligned} F_{Cx} &= \frac{\rho}{2} V_{Cr}^2 B T C_{Cx}(\alpha_C) \\ F_{Cy} &= \frac{\rho}{2} V_{Cr}^2 L_{BP} T C_{Cy}(\alpha_C) \\ N_C &= \frac{\rho}{2} V_{Cr}^2 L_{BP}^2 T C_{Cn}(\alpha_C) \end{aligned} \tag{19}$$

Here; C_{Cx}, C_{Cy}, and C_{Cn} stand for current coefficients. These coefficients for given current directions can be obtained by model tests or CFD analysis. Alternatively, particularly for early design studies, several empirical methods based on the analysis of model test data are available. For example, Remery and Van Oortmerssen (1973) presented an empirical method to predict current forces on tanker shaped hulls based on several model tests. The longitudinal current force is assumed to be due to the frictional resistance and hence could be estimated by the flat plate resistance in accordance with the ITTC formulation. The transverse current force and current yaw moment coefficients were assumed independent of the Reynolds number and expanded in fifth order Fourier series as a function of relative current direction. The average values of the Fourier coefficients were provided. Details of the parameters in this equation and the in-depth methodology can be found in IMCA M140 (2000).

2.7. External disturbances – Wave drift loads

The wave forces acting on the vessel can be classified into two distinct types as the harmonic first order wave forces and the second order mean wave drift forces. Because of the high frequency and the large magnitude of the first order wave forces the thrusters are not capable to counteract these forces. Therefore, only the second order mean wave drift forces need to be considered. The total wave drift force for a given wave direction can be determined from the following equation, API RP 2SK (2005):

$$F_{WDr}(\alpha_{Wr}) = F_{WDy}(90)\left[\frac{2\sin^2(\alpha_{Wr})}{1+\sin^2(\alpha_{Wr})}\right] + F_{WDx}(0)\left[\frac{2\cos^2(\alpha_{Wr})}{1+\cos^2(\alpha_{Wr})}\right] \tag{20}$$

where α_{Wr} stands for relative wave angle, $F_{WDx}(0)$ and $F_{WDy}(90)$ stand for wave drift forces in surge and sway, respectively. The wave drift forces and moment are estimated by using the empirical relation given by DNVGL-ST-0111 (2018).

ISSN: 1300-1973, e-ISSN: 2651-530X, Journal homepage: http://www.gmoshipmar.org/
Research Article

3. Maneuvering Derivatives of the Vessel and Details of CFD implementation

Basic geometric and hydrostatic properties of the vessel are provided by SKIPSTEKNISK. The vessel has single shaft, propeller and rudder. General particulars of the vessel are presented in Table 1 and her profile view in Figure 1.

Table 1: General particulars of the vessel

Length over all	L_{OA}	87.53 m
Length between perpendiculars	L_{BP}	78.60 m
Beam	B	18.00 m
Draught (midship)	T	6.40 m
Draught (AP)	T_A	6.65 m
Draught (FP)	T_F	6.15 m
Displacement	Δ	6500 t
Block coefficient	C_B	0.738
Wetted surface area	S	2110 m^2
Projection area of rudder	A_R	16 m^2
Bilge keel surface area	A_{BK}	42 m^2
Form factor	k	0.41
Frontal wind area	A_{WF}	375 m^2
Transverse wind area	A_{WT}	1160.7 m^2
No of propeller blades	Z	4
Propeller diameter	D	4.5 m
Propeller pitch ratio at 0.7R	P/D	1.2
Expanded blade area ratio	A_E/A_0	0.611

The hydrodynamic coefficients of the trawler are obtained by conducting PMM tests via a RANSE-based CFD on the one hand and by means of empirical formulas on the other.

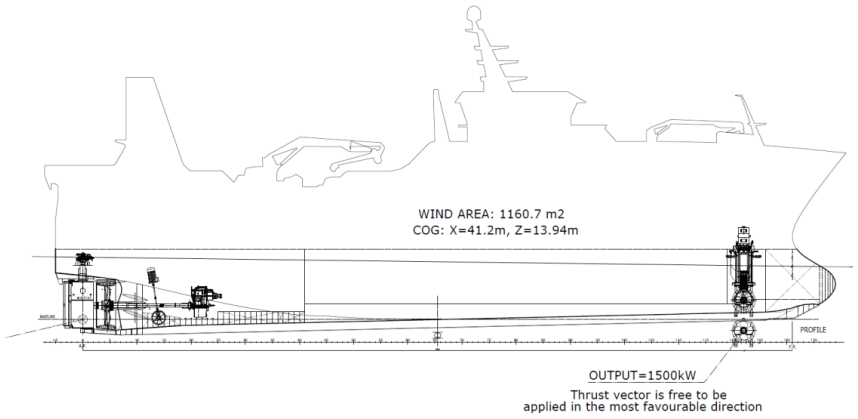

Figure 1. Profile of the stern trawler and the arrangement of the azimuth thruster

3.1. Numerical implementation

A three-dimensional, incompressible and viscous Reynolds-Averaged Navier-Stokes Equations (RANSE) based computational fluid dynamics (CFD) approach is implemented for captive motion tests of the trawler. The flow is turbulent due to high Reynolds number. Realizable k-epsilon is selected as the

turbulence model. Due to low ship speed, a double-body flow model is utilized. Only the underwater hull form is considered while the free water surface boundary condition is selected as “symmetry”. This is to ensure calm water condition during tests (due to low ship speed); therefore, wave resistance is neglected.

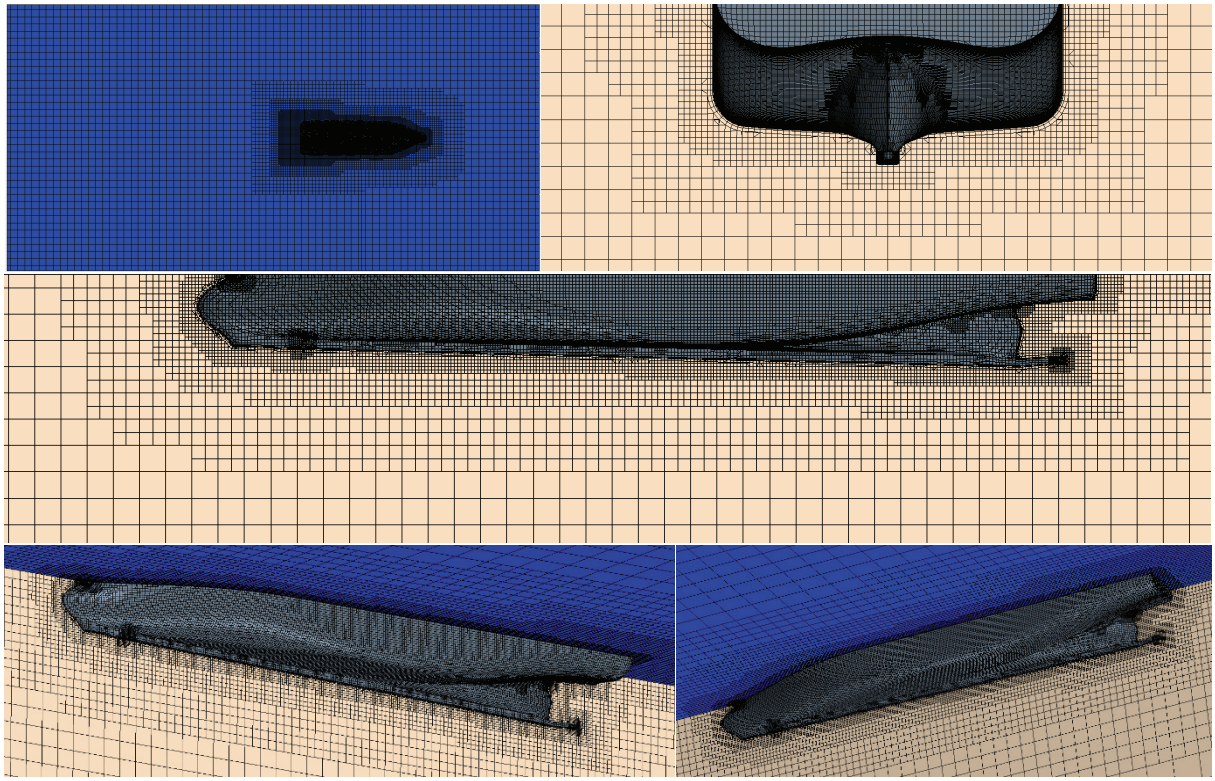

Figure 2. Different views of the grid used in numerical simulations

The underwater form of the trawler is enclosed in a rectangular box. The boundary conditions applied to the six surfaces of this box are explained below:

- The inlet upstream of the trawler: Velocity inlet.
- The outlet downstream of the trawler: Pressure outlet.
- Two side walls (one at the left, the other at the right of the trawler): Velocity inlet.
- The bottom wall: Velocity inlet.
- The top wall: Symmetry (to ensure double-body flow model).

The tests are conducted at 3knots ship speed at full-scale, corresponding to 0.2817m/s for the 1/30 model scale ship. The ship is stationary while a flow velocity of -0.2817m/s is sent from the velocity inlet towards the ship.

Approximately 500k grid elements were used to represent the fluid domain. The cell base size is set to 0.01m. Minimum cell size can get as low as 25% of the base size where refinements are required to solve for high adverse pressure gradients. The maximum cell size is 1600% of the base size and used in inlet, outlet, and side wall surfaces, corresponding to 0.16m. Different views of the grid system implemented in the fluid domain are given in Figure 2. Prism layer thickness is calculated using turbulent boundary layer thickness formula given by

ISSN: 1300-1973, e-ISSN: 2651-530X, Journal homepage: http://www.gmoshipmar.org/
Research Article

$$\delta \approx 0.37 \frac{L}{Re^{0.2}} \tag{21}$$

where δ denotes the boundary layer thickness, L is the ship length and Re is the Reynolds number (Schlichting, 1979). The boundary layer thickness is found to be $\delta = 0.0106m$. It is represented by 3 prism layers only, due to low ship speed. Wall y+ are considered during the selection of the number of prism layers. Wall y+ and the turbulence viscosity ratio contours are given in Figure 3.

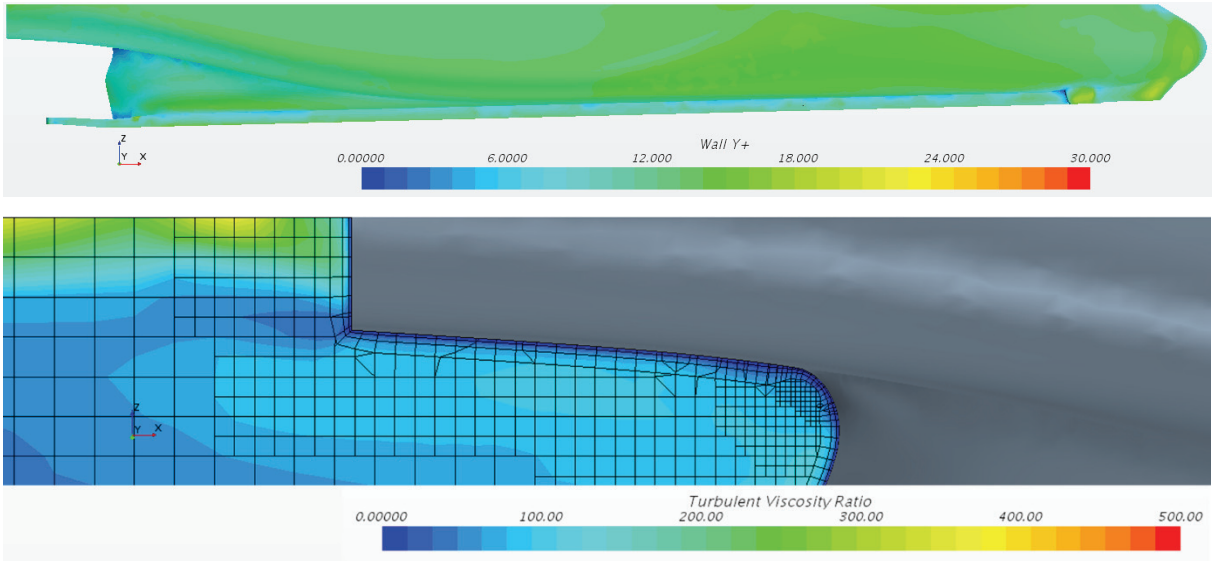

Figure 3. Wall y+ distribution along the ship (top). The turbulence viscosity ratio at the stern region (bottom)

The steady solver is used for static tests (static drift) while the transient solver is selected for dynamic tests (pure yaw, yaw and drift). The time step size is taken as $\Delta t = 0.02s$ in dynamic tests. Maximum inner iterations are set to 5.

3.2. Validation of the numerical approach

Numerical simulations are validated by the frictional resistance coefficient obtained by CFD and comparing it with the ITTC-1957 frictional correlation line formula:

$$C_{F,ITTC} = \frac{0.075}{(\log Re - 2)^2} \tag{22}$$

where Re denotes the Reynolds number. Results are validated for a full-scale velocity of $U_S = 3knots$. The corresponding model velocity at 1/30 model scale is $U_M = 0.2817m/s$ Considering that the model ship has a length of $L = 2.6232m$, the Reynolds number in this case is $Re \approx 830{,}000$. Then, the frictional resistance coefficient becomes $C_{F,ITTC} = 4.88 \cdot 10^{-3}$. CFD simulations are conducted for a full-scale ship velocity range of $1knot < U_S < 8knots$. Results are given in Table 2.

The difference between the two results, around the given operation speed of 3 knots, is only 0.6%, which is considered to be negligible.

Table 2. Comparison of frictional resistance coefficients obtained by CFD and ITTC-1957 formula

U_S	U_S	U_M	Re	C_F $(ITTC)$	R_F $(ITTC)$	R_F (CFD)	C_F (CFD)	Difference
$knots$	m/s	m/s	$-$	$-$	N	N	$-$	%
1	0.5144	0.0939	2.77E+05	6.33E-03	0.0671	0.0646	6.10E-03	3.7
2	1.0288	0.1878	5.53E+05	5.35E-03	0.2269	0.2328	5.49E-03	2.6
3	**1.5432**	**0.2817**	**8.30E+05**	**4.88E-03**	**0.4657**	**0.4683**	**4.91E-03**	**0.6**
4	2.0576	0.3757	1.11E+06	4.59E-03	0.7775	0.7721	4.55E-03	0.7
5	2.5720	0.4696	1.38E+06	4.37E-03	1.1587	1.1399	4.30E-03	1.6
6	3.0864	0.5635	1.66E+06	4.21E-03	1.6065	1.5705	4.12E-03	2.2
7	3.6008	0.6574	1.94E+06	4.08E-03	2.1188	2.0588	3.97E-03	2.8
8	4.1152	0.7513	2.21E+06	3.97E-03	2.6940	2.5903	3.82E-03	3.8

3.3. Numerical PMM test results

Numerical simulations of static drift tests have been conducted for six cases in a range of $0 \leq \beta \leq 15°$. Full-scale ship velocity is $U_S = 3knots$, corresponding to a model ship velocity of $U_M = 0.2817m/s$ (using Froude similarity). Non-dimensional lateral ship velocity can be calculated by $v' = -\sin\beta$. Numerical results are presented in digital form and graphed in Figure 4.

Pure yaw tests have been conducted for eight cases in a range of $0.05 \leq r' \leq 0.4$. Non-dimensional yaw rate denoted by r' is calculated by $r' = \frac{rL}{U}$. Numerical results are given in Figure 5.

Yaw and drift tests have been conducted for four different yaw rates consisting of $r' = 0.1$, $r' = 0.2$, $r' = 0.3$, and $r' = 0.4$. Each one of these cases were simulated for five drift angles in a range of $0 \leq \beta \leq 15°$ (similar to the static drift tests). With the additional case of $\beta = 0$ available from pure yaw tests, a total of 24 numerical simulations were available for this test. Numerical results are given in Figure 6.

4. Turning Performance in Calm Water

In this section turning performance of the Stern Trawler with a trawl pull load of 40 metric tons in calm water conditions is presented. The forward speed of the vessel is 3 knots with a propeller rotation rate of 88 rpm and the maximum rudder angle is 35 degrees.

4.1. Turning circle test without the azimuth thruster

For the base configuration, only the propeller and rudder are taken into consideration. Figure 7 presents the port and starboard turning manoeuvre simulations with

- a trawl pull load of 40 metric tons
- at 3 knots forward speed
- with propeller rotation rate of 88 rpm and
- a rudder angle of 35 degrees.

The total simulation time is 600 seconds with a time step of 15 seconds.

ISSN: 1300-1973, e-ISSN: 2651-530X, Journal homepage: http://www.gmoshipmar.org/
Research Article

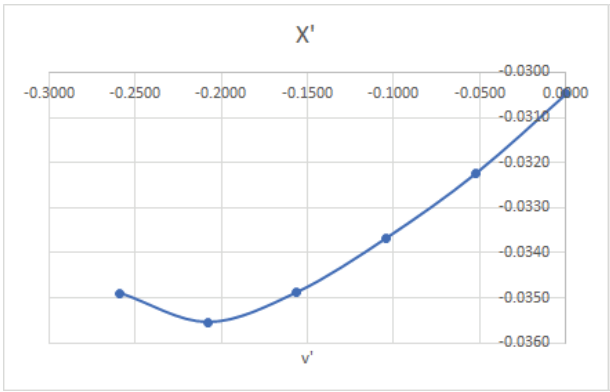

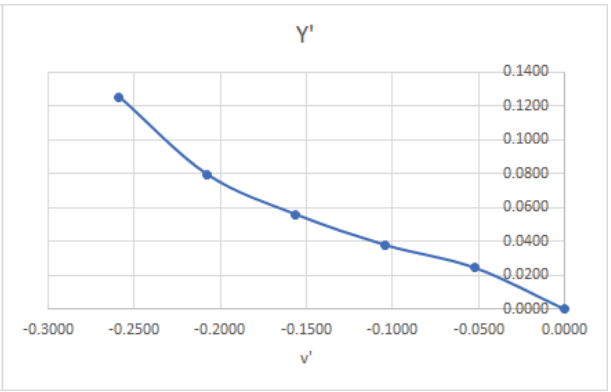

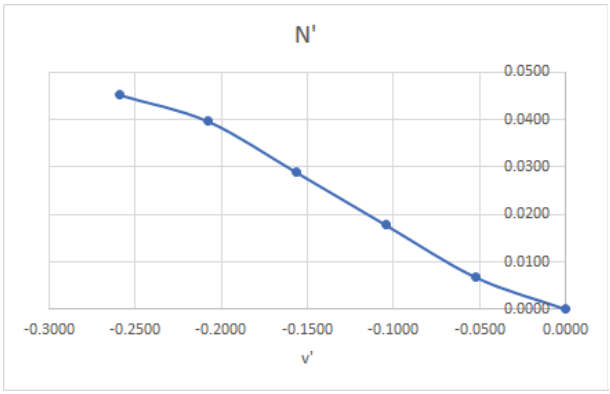

beta	v'	X'	Y'	N'
rad	-	-	-	-
0	0	-0.0305	0	0
0.0524	-0.0523	-0.0322	0.0246	0.0068
0.1047	-0.1045	-0.0337	0.0381	0.0178
0.1571	-0.1564	-0.0349	0.0562	0.0289
0.2094	-0.2079	-0.0355	0.0798	0.0397
0.2618	-0.2588	-0.0349	0.1255	0.0453

Figure 4. Non-dimensional forces (X' and Y') and moment (N') graphs in static drift tests. Tabular version (right below)

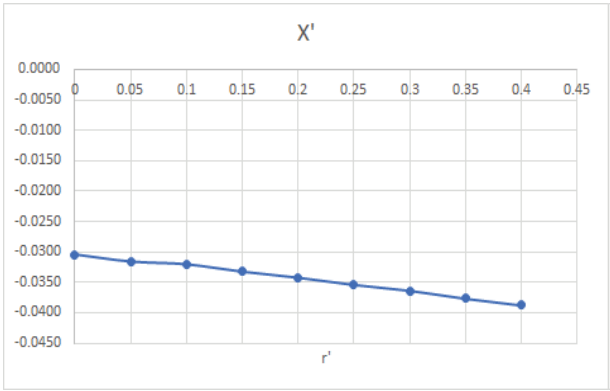

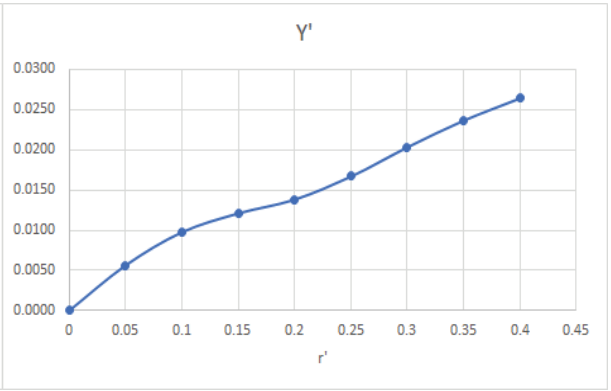

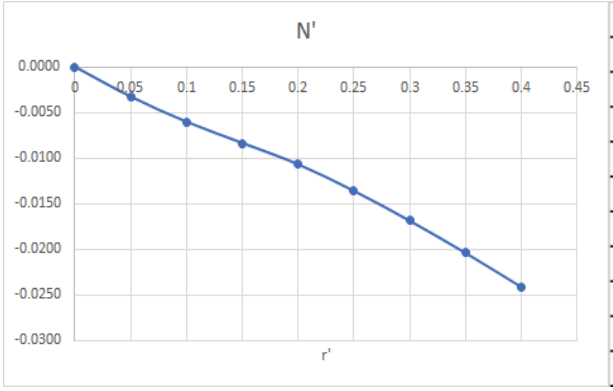

r'	X'	Y'	N'
-	-	-	-
0	-0.0305	0	0
0.05	-0.0316	0.0056	-0.0033
0.1	-0.0321	0.0098	-0.0060
0.15	-0.0333	0.0121	-0.0083
0.2	-0.0342	0.0138	-0.0107
0.25	-0.0354	0.0167	-0.0136
0.3	-0.0364	0.0204	-0.0169
0.35	-0.0377	0.0237	-0.0204
0.4	-0.0388	0.0264	-0.0241

Figure 5. Non-dimensional forces (X' and Y') and moment (N') graphs in pure yaw tests. Tabular version (right below)

4.2. Turning performance with an azimuth thruster

For this configuration, a 1200 kW azimuth thruster located in the forebody is taken into consideration besides the propeller and the rudder. In order to illustrate the effect of the azimuth thruster on the turning performance, two different thrust levels (50 kN and 100 kN) are considered.

Figure 8 presents the turning manoeuvre simulation with

- a trawl pull load of 40 metric tons
- at 3 knots forward speed
- with a propeller rotation rate of 88 rpm
- the rudder angle is 0 degrees
- the direction of the azimuth thrusters 90 degrees

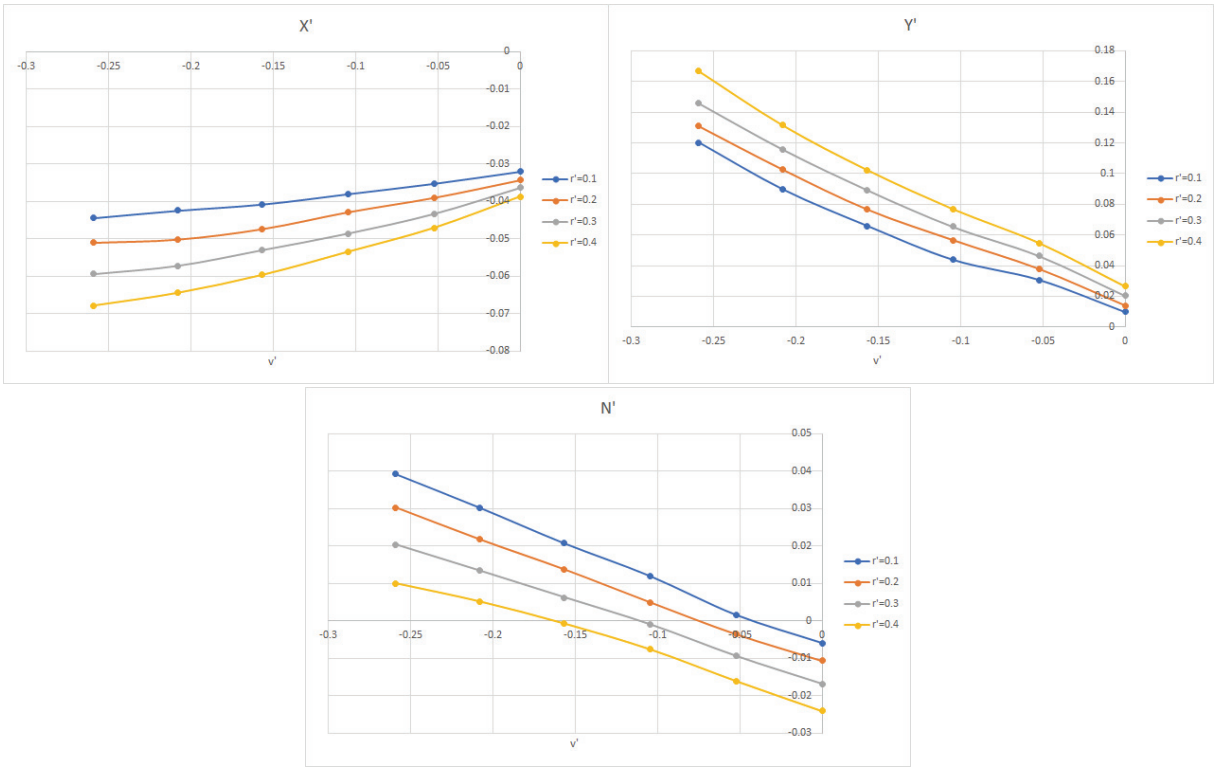

Figure 6. Non-dimensional forces (X' and Y') and moment (N') graphs in yaw and drift tests. Tabular version (right below)

The azimuth thruster provides 50 kN and 100 kN thrust in these simulations. 0 degree represents the vessel's heading and 90 degrees represents the thruster direction perpendicular to the vessel's heading. The total simulation time is 240 seconds with a time step of 10 seconds. The figure shows the effect of the azimuth thruster on the turning performance in calm water conditions.

5. The effect of environmental loads on a ship in surge

In this section, the effect of environmental loads on the vessel's motions are investigated. The vessel is assumed to be subject to surge, sway forces, and yaw moment due to the wind, current and waves. In order to keep station or maintain track, these forces and moment must be compensated by those

ISSN: 1300-1973, e-ISSN: 2651-530X, Journal homepage: http://www.gmoshipmar.org/
Research Article

generated by the propeller, rudder and the thruster. The details of the methods and procedures used to estimate the wind, current and wave forces are presented in Section 2. The wind and wave characteristics for Beaufort 9 (BF 9) condition are determined in accordance with the recommendations of DNV GL ST-0111 (2018) as given in Table 3.

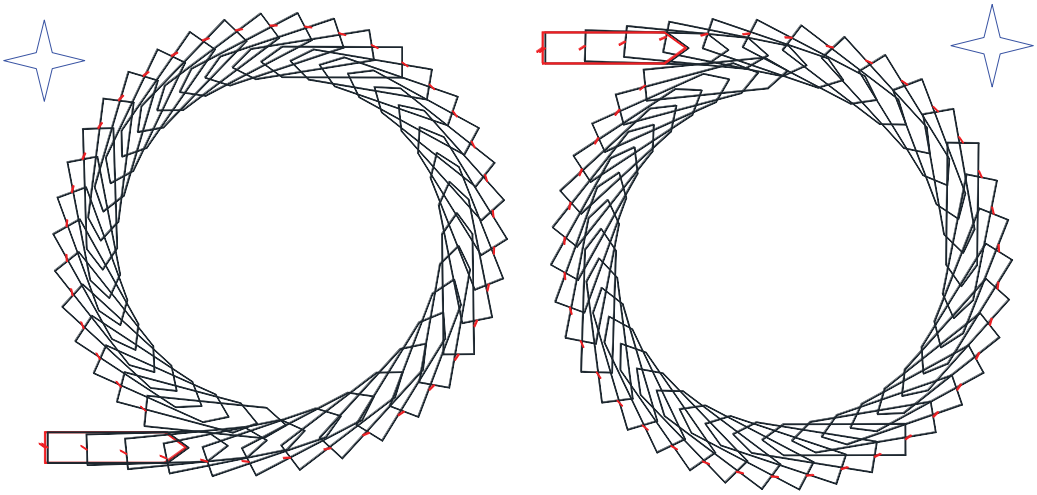

Figure 7. Turning manoeuvre simulation with a trawl pull load of 40 metric tons at 3 knots speed with a rudder angle of 35 degrees to port (left) and starboard (right).

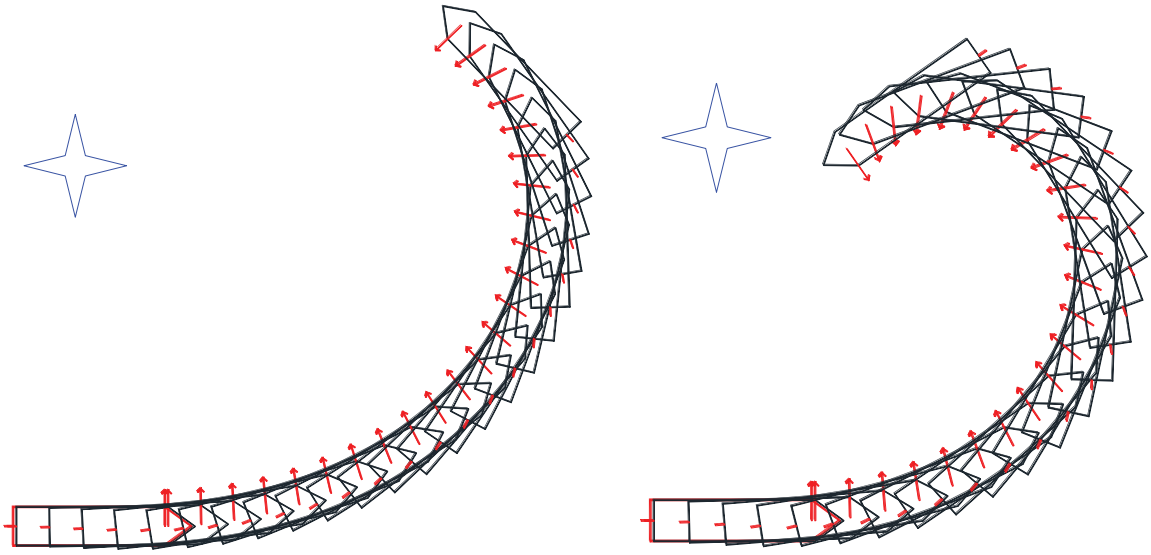

Figure 8. Turning manoeuvre simulation with trawl pull load of 40 metric tons at 3 knots with a rudder angle of 0 degrees. The thrust of the azimuth thruster is 50 kN (left) and 100 kN (right). The direction of the azimuth thruster is 90 degrees.

Table 3. Beaufort 9 sea condition.

Beaufort No	Description	Wind speed [m/s]	Significant wave height [m]	Modal wave period [s]
9	Strong gale	24.4	7.4	10.5

The effect of the environmental loads is considered in this section where the vessel is

- towing a trawl pull load of 40 metric tons
- a steady forward speed of 3 knots
- with a propeller rotational rate of 88 rpm and
- the rudder angle is 0 degrees.

We consider the environmental loads one-by-one in this section and the results obtained for each are presented in the sub-sections below.

5.1. Wind forces

The direction of the wind is perpendicular to the vessel's initial heading. There are no active thrusters other than the propeller. The effect of waves and current are not taken into consideration. Typical examples of manoeuvring simulations based on Isherwood (1994), Blendermann (1994) and DNVGL-ST-0111 (2018) formulations in BF 9 conditions with a wind speed of 24.4 m/s are shown in Figure 9. The total simulation time is 180 seconds and the time interval is 10 seconds. As shown in the figures, different formulations yield similar behaviour of the vessel.

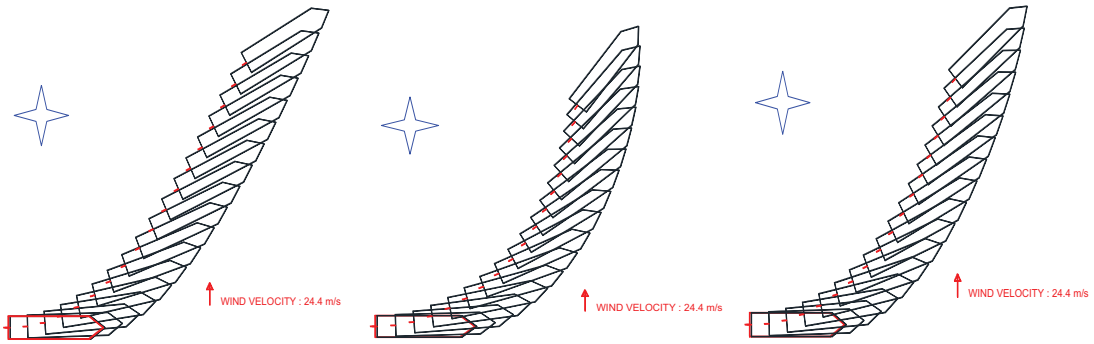

Figure 9. The effect of wind forces (BF 9) on a ship in surge. Isherwood (1994) formulation (left), Blendermann (1994) formulation (middle) and DNVGL-ST (2018) formulation (right).

5.2. Current forces

The direction of the current is perpendicular to the vessel's heading. There are no active thrusters other than the propeller. The current velocity is 3knots. The effect of wind and waves are not taken into consideration. Typical examples of manoeuvring simulations based on Remery and Van Oortmerssen (1973), Nienhuis (1987), API RP 2SK (2005), IMCA M140 (2000) and DNVGL-ST-0111 (2018) formulations are shown in Figure 10. The total simulation time is 180 seconds and the time interval is 10 seconds.

5.3. Wave drift forces

As explained in Section 2.8, only the second order mean wave drift forces need to be taken into account. Wave drift forces are estimated by the empirical method recommended by DNVGL-ST-0111 (2018). This method considers the wave period which has strong influence on wave drift predictions. Figure 11 illustrates the wave drift effect in BF 9 conditions with a significant wave height of 7.4 m.

ISSN: 1300-1973, e-ISSN: 2651-530X, Journal homepage: http://www.gmoshipmar.org/
Research Article

Direction of waves is perpendicular to the vessel's heading. There are no active thrusters other than the propeller. The effect of wind and current are not taken into consideration.

In the following sections the effect of the azimuth thruster on manoeuvring performance of the vessel is investigated by simulating the beahaviour of the vessel under the effects of wind, waves and current. In order to provide objective comparisons the wind, current and wave drift loads are estimated by DNVGL-ST-0111 (2018) formulations.

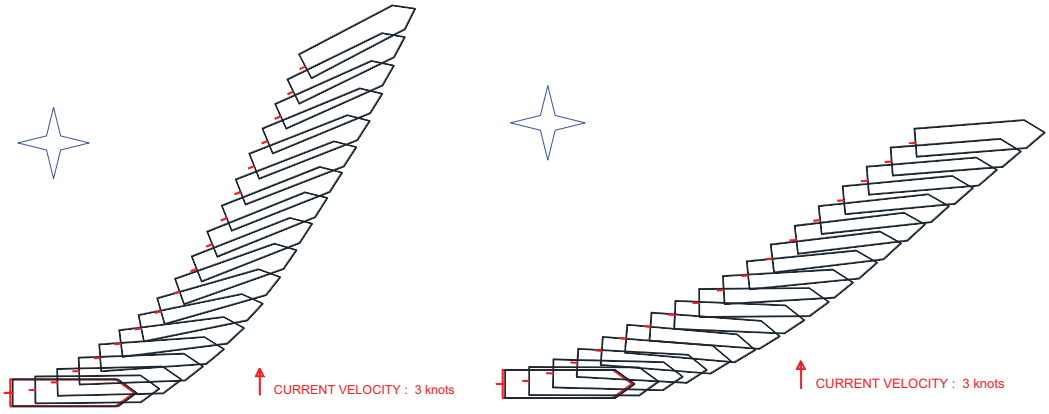

Figure 10. The effect of current forces on a ship in surge. From the left: IMCA M140 (2000), and DNVGL-ST-0111 (2018) formulations.

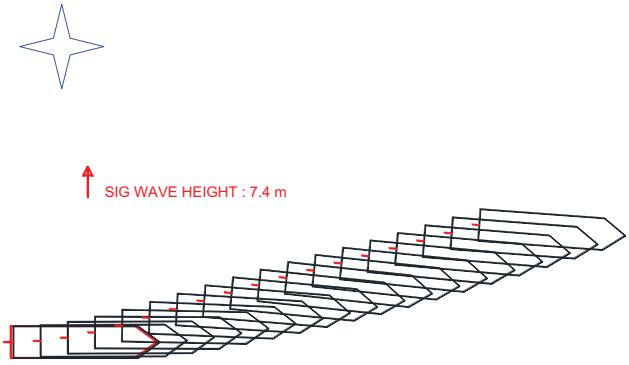

Figure 11. The effect of wave drift forces with DNVGL-ST-0111 (2018) formulation

6. The Efficiency of the Azimuth Thruster in BF 9 Conditions

It is shown in Section 4 that the azimuth thruster located in the forward part of the vessel is very effective in calm water conditions while the vessel is towing a trawl net of 40 metric tons with a steady speed of 3 knots. In Section 5, the environmental loads due to wind, current and waves in BF9 conditions are estimated. This section presents the results of manoeuvring simulations with the azimuth thruster under the influence of wind, current and waves in BF9 conditions. The trawler speed is 3 knots and the propeller rotation rate is 88 rpm, unless stated otherwise.

6.1. Keeping track against wind loads

In this section, we illustrate the efficiency of the azimuth thruster in keeping track at 3 knots forward speed with a trawl pull load of 40 metric tons against wind forces and moment in BF 9 conditions with

a mean wind speed of 24.4 m/s. The wind direction is perpendicular to vessel's heading. The total simulation time is 180 seconds and the time interval is 10 seconds.

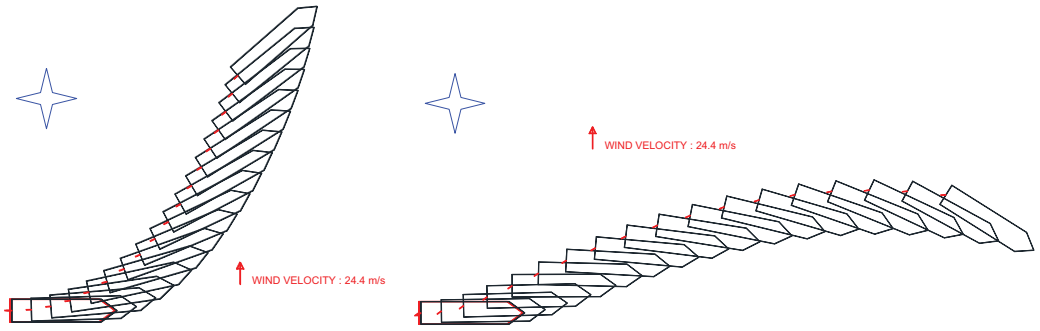

Rudder = 0 deg, Thruster =0 kN, Propeller = 88 rpm Rudder = 35 deg, Thruster = 0 kN, Propeller = 100 rpm

Figure 12. The effect of the propeller and the rudder in BF9 conditions using DNVGL-ST-0111 (2018) formulation. The speed increases with increasing propeller rotation rate.

Figure 12 shows a comparison of the behaviour of the vessel in BF 9 conditions at neutral rudder angle (left) and with a rudder angle of 35 degrees (right). Current and wave effects are ignored and the wind forces are estimated by DNVGL-ST-0111 (2018) formulation. As shown in the figure, the propeller rate of rotation (88 rpm) and the forward speed of 3 knots are too low for the rudder to be effective. When the propeller rate of rotation is increased to 100 rpm the rudder becomes effective on controlling the vessels's heading against the wind. However, due to the increase in the propeller rate of rotation, forward speed of the vessel increases to 6 knots. Figure 13 shows the effect of azimuth thruster on keeping track against the wind. The thrust is increased up to 130 kN with constant thruster angle of 90 degrees (perpendicular to vessel heading).

The azimuth thruster needs a thrust more than 100 kN to counteract the environmental loads on the ship, as Figure 13 shows.

The results indicate that in order to maintain track against wind loads in mean BF 9 conditions, at least 120-150 kN thrust is required for this ship. The effectiveness of the rudder at 3 knots forward velocity is negligible. The propeller rate of rotation needs to be increased for the rudder to be effective, resulting in an increase in the forward velocity.

6.2. Keeping track against current loads

In this section, the efficiency of the azimuth thruster in keeping track

- with a trawl pull load of 40 metric tons
- at 3 knots forward speed and
- a propeller rotation rate of 88rpm

against current forces with a mean current velocity of 3 knots is illustrated. The current direction is perpendicular to vessel's heading.

ISSN: 1300-1973, e-ISSN: 2651-530X, Journal homepage: http://www.gmoshipmar.org/
Research Article

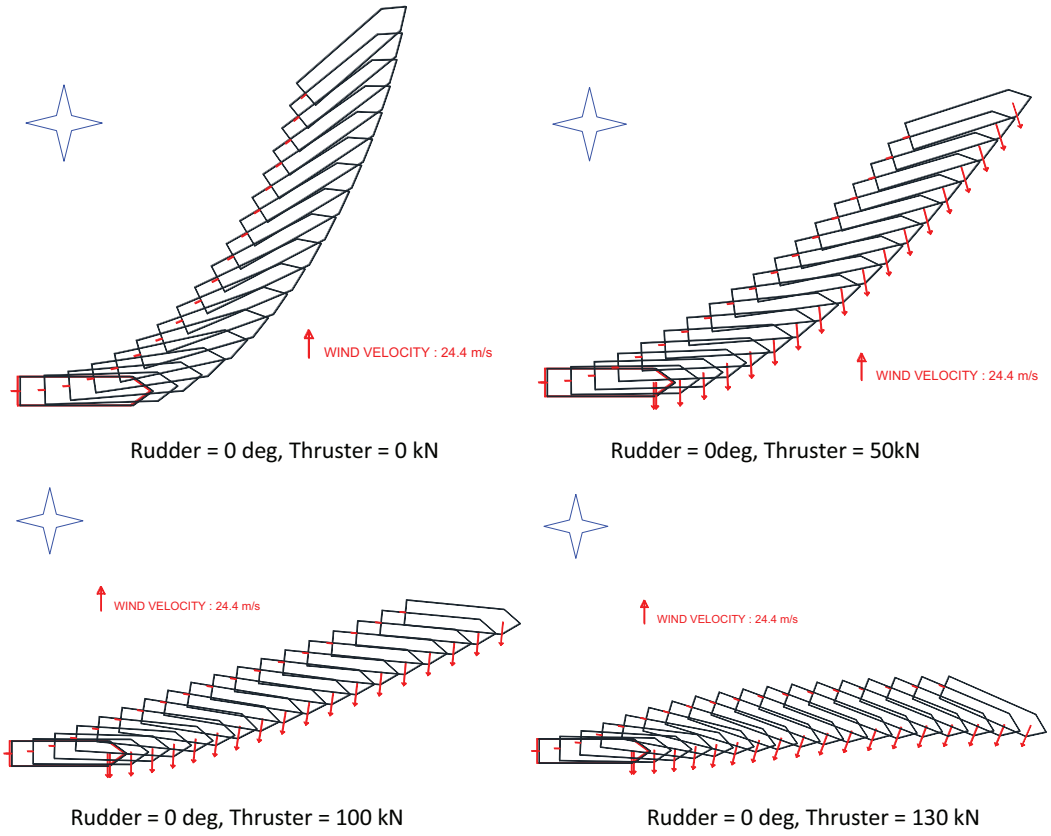

Figure 13. The effect of the azimuth thruster in BF 9 conditions using DNVGL-ST-0111 (2018)

Figure 14 shows a comparison of the behaviour of the vessel in uniform current with a mean velocity of 3 knots with neutral rudder angle (left) and with a rudder angle of 35 degrees (right). The azimuth thruster produces zero net force in these simulations. Wind and wave effects are ignored and the current forces and moment are estimated by DNVGL-ST-0111 (2018) formulation. As shown in the figure, the propeller rotataion rate at 88 rpm and the forward ship speed at 3 knots are too low for the rudder to be effective. When the propeller rotation rate is increased to 100 rpm, the rudder becomes effective on controlling the vessels's heading against the current. However, due to the increase in the propeller rate of rotation, forward speed of the vessel increases to 6 knots.

Figure 15 shows the effect of the azimuth thruster on keeping track against the current. The thrust is increased from 50 kN to 100 kN at a constant thruster angle of 90 degrees (perpendicular to vessel heading). The present computations also showed that the response of the ship is much better when the azimuth thruster and the rudder work together (despite a decrease in the thruster angle).

These results indicate that in order to maintain track against current loads due to a 3 knots uniform current, at least 100-120 kN thrust is required. The effectiveness of the rudder at 3 knots forward velocity is negligible and for the rudder to be effective the propeller rate of rotation needs to be increased resulting in an increase in the forward velocity.

6.3. Keeping track against wave drift loads

The efficiency of the azimuth thruster in keeping track against wave drift loads is presented in this section. The ship is moving forward

- with a trawl pull load of 40 metric tons
- at 3 knots forward speed and
- a propeller rotation rate of 88rpm

against wave drift forces and moment in mean BF 9 conditions with a significant wave height of 7.4 m. The wave direction is perpendicular to vessel's heading. Wind and current effects are ignored and the wave drift forces and moment are estimated by DNVGL-ST-0111 (2018) formulation. The total simulation time is 180 seconds and the time interval is 10 seconds. Results with and without the azimuth thruster are given in Figure 16.

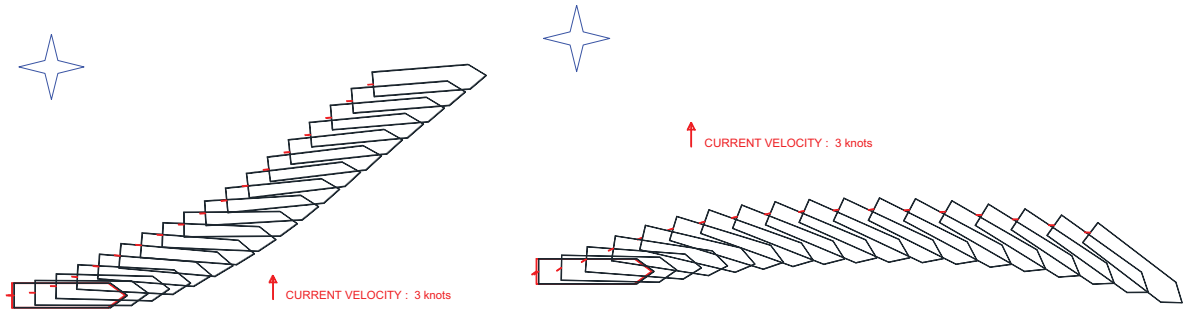

Rudder = 0 deg, Thruster =0 kN, Propeller = 88 rpm Rudder = 35 deg, Thruster = 0 kN, Propeller = 100 rpm

Figure 14. The response of the ship to current loads without the azimuth thruster using DNVGL-ST-0111 (2018) formulation

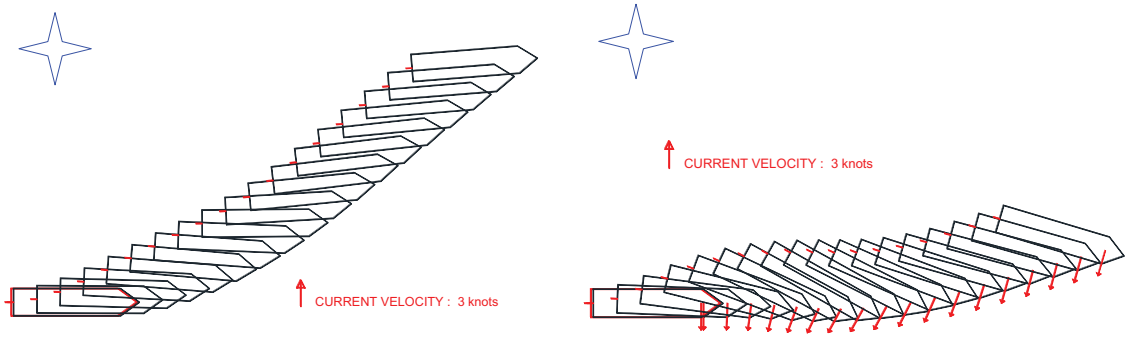

Rudder = 0 deg, Thruster =0 kN Rudder = 0 deg, Thruster = 100 kN, Thruster angle = 90 deg

Figure 15. The response of the ship to current loads with the azimuth thruster using DNVGL-ST-0111 (2018) formulation.

These results indicate that the ship can maintain its course in waves without the thruster but the sway distance is considerably high. With

- an azimuth thruster providing 50 kN thrust
- at an angle of 60 degrees and
- a rudder at 35 degrees,

the sway translation distance of the ship can be limited.

ISSN: 1300-1973, e-ISSN: 2651-530X, Journal homepage: http://www.gmoshipmar.org/
Research Article

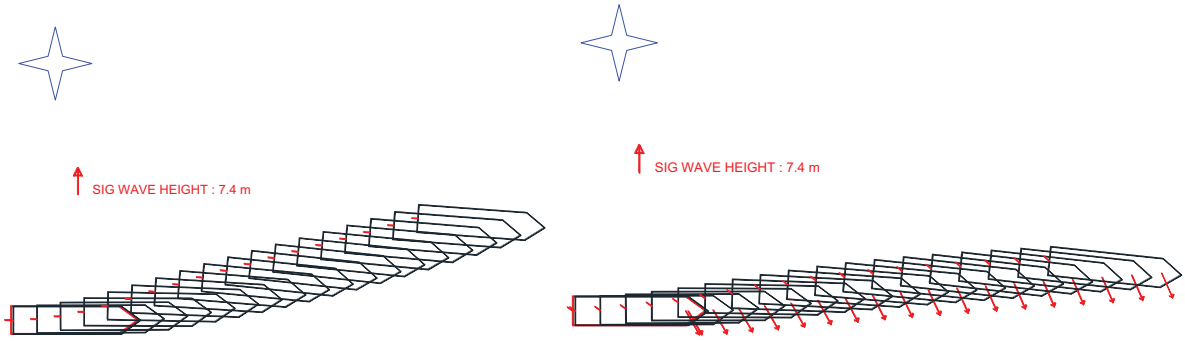

Rudder = 0deg, Thruster =0kN Rudder = 35deg, Thruster = 50kN, Thruster angle = 60deg

Figure 16. Ship response to wave drift loads using DNVGL-ST-0111 formulation in BF 9.

7. Maximum environmental conditions for keeping track

This section presents maximum wave, wind and current conditions in which the vessel is able to keep track with an azimuth thruster of about 175 kN effective thrust (205 kN nominal thrust) capacity. Depending on the current velocity, four cases are considered in the following sub-sections. Wind, current and wave drift forces are estimated by DNVGL-ST-0111 (2018) formulations. The wind and wave characteristics for Beaufort 6-9 (BF 6-9) conditions are determined in accordance with the recommendations of DNV GL ST-0111 (2018) as given in Table 4.

Figure 17 presents various environmental scenarios and the required thrust for the vessel to maintain its course. The efficiency of the azimuth thruster in keeping track

- with a trawl pull load of 40 metric tons
- at 3 knots forward speed
- a propeller rotation rate of 88rpm

against wind and wave forces and moment is evaluated. In this figure, the ship cannot keep its track when the required thruster force is above 175 kN.

Table 4. Definition of sea conditions in Beaufort scale.

Beaufort No	Description	Wind speed [m/s]	Significant wave height [m]	Modal wave period [s]
6	Strong breeze	13.8	3.1	8.5
7	Moderate gale	17.1	4.2	9.0
8	Gale	20.7	5.7	10.0
9	Strong gale	24.4	7.4	10.5

8. Summary of Results and Conclusions

In this paper, results of computational analyses on the manoeuvring performance of astern trawler are presented. The manoeuvring performance of the vessel is assessed and simulated for two different configurations with a ship forward speed of 3 knots and a trawl pull load of 40 metric tons in calm

water and Beaufort 9 environmental conditions. The first configuration considers the propeller and the rudder only while the second configuration also takes into account an azimuth thruster installed in the fore body.

First, the manoeuvring derivatives are computed by empirical and CFD based methods and the manoeuvring equations of motion are set. The external forces due to the propeller, rudder and the azimuth thruster are estimated by suitable semi-empirical methods. Several empirical methods to estimate the environmental forces due to wind, waves and current are compared and DNVGL-ST-0111 (2018) formulation is selected as the standard method.

In Base Case (1) configuration, the vessel is fitted with an azimuth thruster in the forebody. The nominal thrust of this thruster at full power is specified as 205 kN by the manufacturer. Because of the thrust losses due to the thruster-hull interaction, current and ventilation effects the actual thrust is estimated to be limited to about 175 kN.

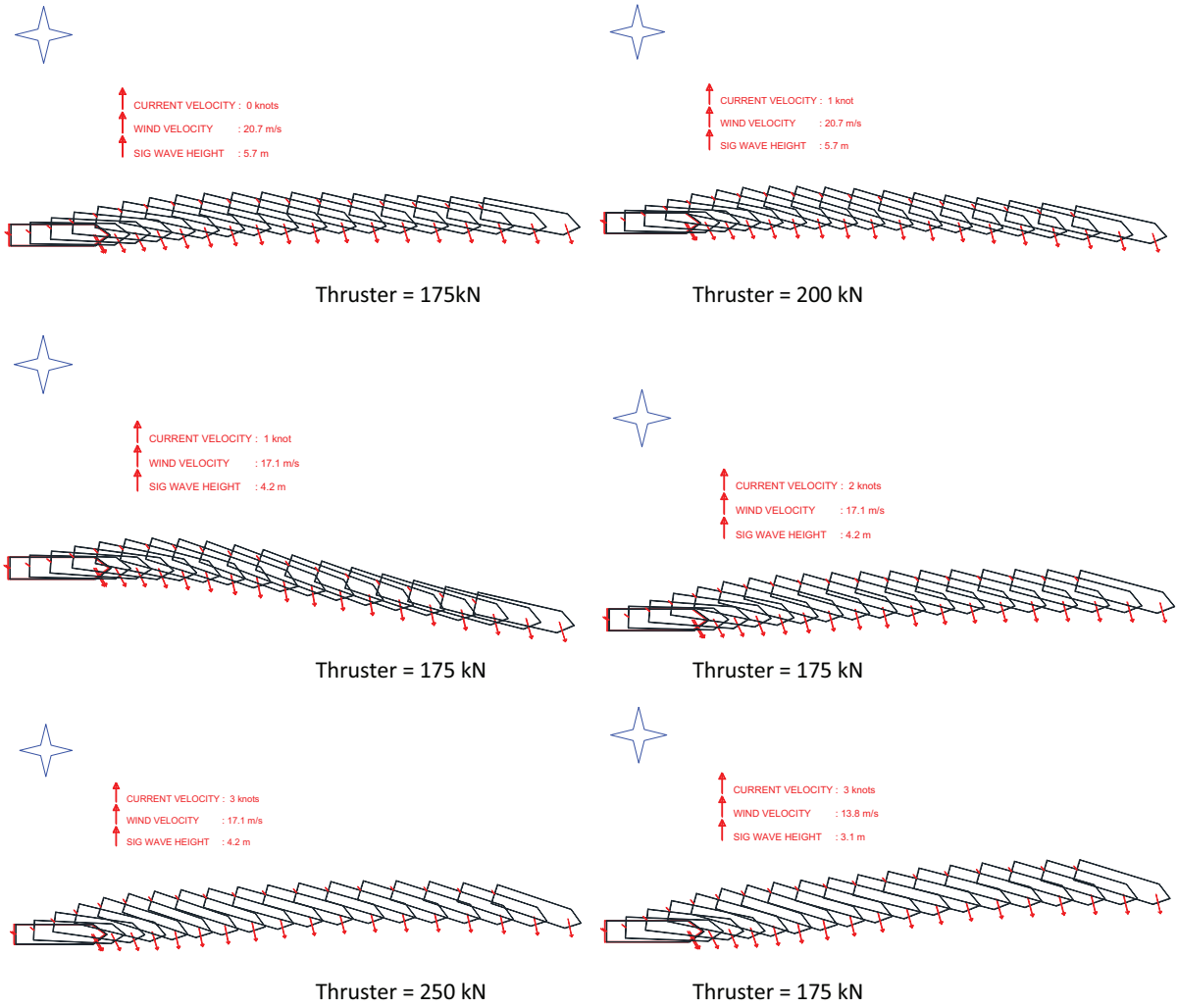

Figure 17. Ship motion response under different environmental conditions. The rudder is at 35 degrees and the thruster angle is 60 degrees in all simulations.

In calm water conditions at 3 knots forward speed (propeller rpm 88) with a trawl pull load of 40 metric tons it is shown that the turning ability of the vessel with 35-degree rudder angle is satisfactory. However, in BF 9 conditions with a mean wind speed of 24.4 m/s the rudder becomes ineffective at

ISSN: 1300-1973, e-ISSN: 2651-530X, Journal homepage: http://www.gmoshipmar.org/
Research Article

keeping track or turning the vessel. Similar effect is observed with increasing wave height and current velocity. The rudder efficiency in rough weather conditions could be increased by increasing the propeller rpm resulting in an increased ship forward speed. However, the focus of this study is the manoeuvring performance at 3 knots forward speed with a trawl pull load of 40 metric tons. Hence, the propeller rpm is assumed to be constant at 88 rpm while considering many of the cases with the environmental loads.

In BF 9 conditions with a wind speed of 24.4 m/s (current and wave effects are ignored) it is estimated that in order to maintain track against wind loads at least 120-150 kN thrust is required. When the combined effects of wind and significant wave height of 7.4 m are taken into consideration, the required minimum thrust of the azimuth thruster increases. Due to the thrust losses the actual thrust is estimated to be limited to about 175 kN. Therefore, it is concluded that the proposed azimuth thruster could not be able to produce sufficient thrust to keep track in BF 9 wind and wave conditions even without current effects. Further analyses have been carried out to consider the maximum environmental conditions in which the vessel could maintain track by using the azimuth thruster. It was found that the ship can maintain its course at a maximum of BF 8 with the azimuth thruster when the wind, wave and current loads are combined.

Acknowledgement

The present work is supported by Skipsteknisk, Türkiye.

References

API RP 2SK, (2005) "*Design and Analysis of Stationkeeping Systems for Floating Structures – Recommended Practice",* American Petroleum Institute (API), Third Edition, October 2005.

Blendermann, W. (1994) "*Parameter Identification of Wind Loads on Ships",* Journal of Wind Engineering and Industrial Aerodynamics, Vol 51, pp 339-351.

DNVGL-ST-0111, (2018) "*Assessment of Station Keeping Capability of Dynamic Positioning Vessels",* DNV-GL, 2018.

IMCA M140, (2000) "*Specification for DP Capability Plots",* The International Marine Contractors Association, June 2000.

Inoue S., Hirano M. and Kijima K., (1981) "*Hydrodynamic Derivatives on Ship Manoeuvring",* International Shipbuilding Progress, Vol. 28, No 321.

Isherwood. R. M., (1972) "*Wind Resistance of Merchant Ships",* Transactions of RINA, Vol. 115, pp 327-338.

Kim, S.-H., Lee, C.-K. and Lee, S.-M. (2021) "*Estimation of Maneuverability of Fishing Vessel Considering Hull-Form Characteristics"*, J. Marine Science and Eng., 9, 569

Nienhuis. U., (1987) "*Simulations of Low Frequency Motions of Dynamically Positioned Offshore Structures",* Transactions of RINA, Vol. 129.

OCIMF 94, (1994) "*Prediction of Wind and Current Loads on VLCCs",* Oil Companies International Marine Forum (OCIMF), Second Edition.

Remery G. F. M. and van Oortmerrsen G., (1973) "*The Mean Wave, Wind and Current Forces on Offshore Structures and their Role in the Design of Mooring Systems",* Offshore Technology Conference, Paper Number OTC 1741, 1973.

Schlichting, H., (1979) "Boundary-Layer Theory*",* 7th edition McGraw-Hill.

Yasukawa, H., & Yoshimura, Y. (2015). Introduction of MMG standard method for ship maneuvering predictions. Journal of Marine Science and Technology, 20(1), 37-52.

Yoshimura, Y. and Ma, N. (2003) "*Manoeuvring Prediction of Fishing Vessels*", MARSIM'03, Conf. Proc., pRC-29-1-10, 25-28 Aug. 2003, Kanazawa, Japan.